A New Approach to Subband Adaptive Filtering

S. Sandeep Pradhan and V. U. Reddy, *Fellow, IEEE*

***Abstract*— Subband adaptive filtering has attracted much attention lately. In this paper, we propose a new structure and a new formulation for adapting the filter coefficients. This structure is based on polyphase decomposition of the filter to be adapted and is independent of the type of filter banks used in the subband decomposition. The new formulation yields improved convergence rate when LMS algorithm is used for coefficient adaptation. As we increase the number of bands in the filter, the convergence rate increases and approaches the rate that can be obtained with a flat input spectrum. The computational complexity of the proposed scheme is nearly the same as that of the fullband approach. Simulation results are included to demonstrate the efficacy of the new approach.**

***Index Terms*— Acoustic echo cancellation, adaptive filtering, subband filtering.**

I. Introduction

A COMMON problem encountered in telephone communication is the presence of echo, which is produced when the signal passes through telephone channels. Removal of this echo requires precise knowledge of the channel, which may be time varying. This calls for adaptive estimation of the channel, which is characterized by time varying impulse response. In recent years, there has been a marked interest in the application of adaptive filtering to acoustic echo cancellation where the impulse response involved is long. We briefly describe this application to motivate our study.

In hands-free telephone sets and teleconferencing systems, both ends of the telephone line consist of audio terminals (see Fig. 1). The received speech signal $y(n)$ is fed to a loudspeaker (LS), which radiates acoustic waves. These waves are fed back to the remote user through the microphone (MP) and constitute the so-called echo. To cancel this echo, we take a sample of $y(n)$, modify it by passing it through an adaptive filter $\hat{S}(z)$, and subtract the resulting signal from $z(n)$. $\hat{S}(z)$ is the estimate of the impulse response of the path that the signal $y(n)$ takes to form the echo $z(n)$. For complete cancellation of this echo, the impulse response of the adaptive filter $\hat{S}(z)$ may have to be very long [1]–[4].

In the above example, the adaptation of the filter is based on the error signal $e(n)$. The algorithm used for adaptation

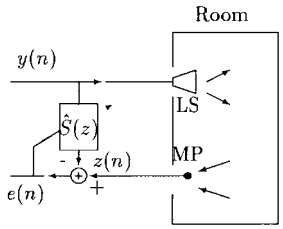

Fig. 1. Acoustic echo canceler.

is generally a gradient type [5]–[7]. The least mean square (LMS) algorithm of Widrow *et al.* [8] has been used widely in such applications. However, it suffers from slow convergence when the input signal to the adaptive filter is correlated, which is generally the case in the above problem. In addition, the convergence performance depends on the length of the filter: the longer the filter, the slower the convergence. Thus, in such applications, the convergence rate of the adaptive filter is the major issue.

Several approaches based on subband adaptive filtering have been recently proposed for the above problem. In these approaches, the underlying signals are decomposed into slightly overlapping frequency bands by passing through a filter bank and the output signals are decimated to give subband signals. Now, the adaptations are carried out in each subband, but the problem with this approach is the aliasing of the input signals, which arises because of the decimation. Several solutions to this problem, such as oversampling [9] of the analysis bank outputs, incorporating adaptive cross filters [10] between the adjacent subbands, and putting spectral gaps between the bands [11], have been recently proposed. In [10], it is pointed out that in the M-band adaptive filters with critical sampling, the cross filters can be avoided if the analysis filters are either ideal filters, or the path impulse response is nonzero for the coefficient indices that are multiples of M and zero otherwise. Thus, the cross filters are unavoidable in practical applications. It has been found [10] that the convergence performance with the cross filters is not better than that of fullband adaptive filter. However, this approach yields a slight gain in computation.

In this paper, we present a new structure for the subband adaptive filter (SAF) with critical sampling and a new criterion for the adaptation algorithm that results in significant improvement in the convergence rate when the LMS algorithm is used for adaptation. This structure exploits the polyphase decomposition of the adaptive filter. To prevent any distortion that may be introduced in splitting and recombining the signals, we use perfect reconstruction filter banks. All the filters used here are real. In our presentation, we consider the problem from the system identification point of view.

Manuscript received January 23, 1996; revised August 3, 1998. The associate editor coordinating the review of this paper and approving it for publication was Dr. Akihiko Sugiyama.

S. Pradhan was with Electrical Communication Engineering Department, Indian Institute of Science, Bangalore, India. He is now with Beckman Institute and Department of Electrical and Computer Engineering, University of Illinois at Urbana-Champaign, Urbana, IL 61801 USA.

V. U. Reddy is with Electrical Communication Engineering Department, Indian Institute of Science, Bangalore, India.

Publisher Item Identifier S 1053-587X(99)01331-8.

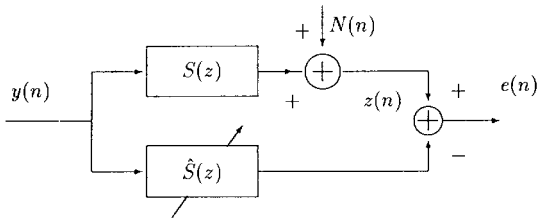

Fig. 2. System identification model.

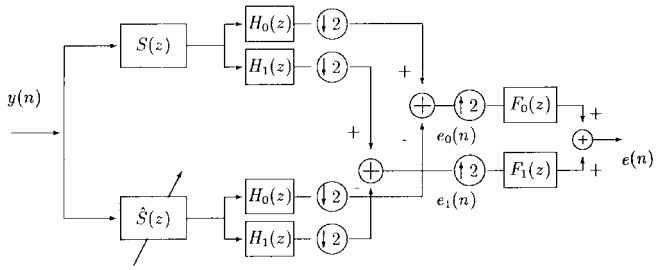

Fig. 3. Equivalent structure of Fig. 2.

The paper is organized as follows. In Section II, we develop and analyze the SAF for the two-band case. The new structure and the new criterion, and hence, the modified LMS algorithm are presented here. Section III extends the proposed approach to the M-band case. Section IV discusses the improvements in the convergence speed that the new approach yields as well as the issues related to the computational complexity. In Section V, we present some simulation results to demonstrate the convergence performance of the proposed approach. The performance of the SAF in the presence of additive noise is also brought out here. Finally, Section VI concludes the paper.

II. Development and Analysis of SAF for 2-Band Case

Consider the system identification model of the echo cancellation problem as shown in Fig. 2. The input signal passes through $S(z)$, which may be unknown and/or slowly varying. The output of this system is corrupted by a signal $N(n)$, which is the system noise in acoustic echo canceler. To estimate this unknown/time varying system, the input is passed through a synthetic filter $\hat{S}(z)$ whose coefficients are adapted in such a way that the power of the error signal $e(n)$ is minimized.

A. Structure of the SAF

An equivalent structure of the above system identification model is given in Fig. 3. Here, the output signals from the filters $S(z)$ and $\hat{S}(z)$ are divided into subbands, decimated, subtracted, and combined through an appropriate filter bank to form the error signal $e(n)$. The signal $N(n)$ is not shown here; we do not consider it in the analysis of the SAF, but its effect on the performance of the SAF will be studied through simulations in Section V. $H_0(z)$ and $H_1(z)$ are the analysis filters, and $F_0(z)$ and $F_1(z)$ are the synthesis filters. These filters form a perfect reconstruction pair. We used cosine modulated paraunitary filter banks in our simulations, although the paraunitary property is not needed for our development and analysis.

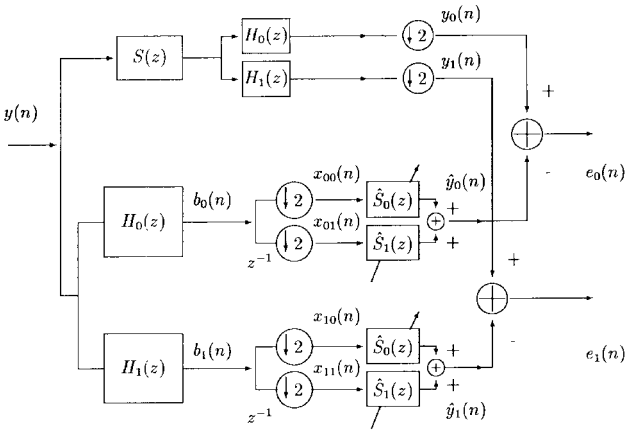

Fig. 4. New structure for the SAF for the two-band case.

Consider $\hat{S}(z)$. It can be decomposed into polyphase components as

$$\hat{S}(z) = \hat{S}_0(z^2) + z^{-1}\hat{S}_1(z^2). \tag{2.1}$$

Using this decomposition and Noble identities [12], the configuration of Fig. 3 can be transformed into Fig. 4. Note that $x_{00}(n)$, $x_{01}(n)$, $x_{10}(n)$, and $x_{11}(n)$ are the subband components of the input $y(n)$, and together, they account for all the samples of $b_0(n)$ and $b_1(n)$, which are the outputs of the filters $H_0(z)$ and $H_1(z)$, respectively. Note also that the cross filters are totally avoided in our structure. However, we have two copies of $\hat{S}_0(z)$ and $\hat{S}_1(z)$, each of length $L/2$, where L denotes the length of $\hat{S}(z)$.

B. Adaptive Algorithm

The filters $\hat{S}_0(z)$ and $\hat{S}_1(z)$ are to be adapted. We use $e_0(n)$ and $e_1(n)$ to adapt the coefficients of these filters. From Fig. 4, we have

$$E_0(z) = Y_0(z) - X_{00}(z)\hat{S}_0(z) - X_{01}(z)\hat{S}_1(z) \tag{2.2}$$

and

$$E_1(z) = Y_1(z) - X_{10}(z)\hat{S}_0(z) - X_{11}(z)\hat{S}_1(z). \tag{2.3}$$

Note that when the spectrum of $y(n)$ is flat, the power of $b_0(n)$ is equal to that of $b_1(n)$, assuming that the filters $H_0(z)$ and $H_1(z)$ are of equal bandwidth with identical passband responses. When $y(n)$ is colored, the power of $b_0(n)$ will be different from that of $b_1(n)$. We define a cost function as

$$J(n) = E(\alpha_0 e_0^2(n) + \alpha_1 e_1^2(n)) \tag{2.4}$$

where α_0 and α_1 are proportional to the inverse of the powers of $b_0(n)$ and $b_1(n)$, respectively, and $E(\cdot)$ denotes the expectation operator. This cost function gives higher weight to the error corresponding to the subband of lower signal power. As we show later in Section IV, this cost function brings down the eigenvalue spread of the weighted sum of the correlation matrices of the input signals to the adaptive filter, thereby resulting in improved rate of convergence.

The gradient-based algorithm for adaptation is given by

$$\hat{s}_{0k}(n+1) = \hat{s}_{0k}(n) - \mu \frac{\partial J}{\partial \hat{s}_{0k}} \qquad k = 0, 1, \cdots, \frac{L}{2} - 1 \tag{2.5}$$

$$\hat{s}_{1k}(n+1) = \hat{s}_{1k}(n) - \mu \frac{\partial J}{\partial \hat{s}_{1k}}, \qquad k = 0, 1, \cdots, \frac{L}{2} - 1 \tag{2.6}$$

where $\hat{s}_{0k}(n)$ and $\hat{s}_{1k}(n)$ are the kth coefficients of $\hat{S}_0(z)$ and $\hat{S}_1(z)$, respectively, at the nth iteration, and μ is the step size. From the cost function (2.4), we have

$$\frac{\partial J}{\partial \hat{s}_{0k}} = 2\alpha_0 E\left(e_0(n)\frac{\partial e_0(n)}{\partial \hat{s}_{0k}}\right) + 2\alpha_1 E\left(e_1(n)\frac{\partial e_1(n)}{\partial \hat{s}_{0k}}\right) \tag{2.7}$$

$$\frac{\partial J}{\partial \hat{s}_{1k}} = 2\alpha_0 E\left(e_0(n)\frac{\partial e_0(n)}{\partial \hat{s}_{1k}}\right) + 2\alpha_1 E\left(e_1(n)\frac{\partial e_1(n)}{\partial \hat{s}_{1k}}\right). \tag{2.8}$$

The partial derivatives of $E_0(z)$ and $E_1(z)$ with respect to $\hat{s}_{0k}$ and $\hat{s}_{1k}$ are given by

$$\frac{\partial E_0(z)}{\partial \hat{s}_{0k}} = -X_{00}(z)z^{-k} \tag{2.9}$$

$$\frac{\partial E_1(z)}{\partial \hat{s}_{0k}} = -X_{10}(z)z^{-k} \tag{2.10}$$

$$\frac{\partial E_0(z)}{\partial \hat{s}_{1k}} = -X_{01}(z)z^{-k} \tag{2.11}$$

$$\frac{\partial E_1(z)}{\partial \hat{s}_{1k}} = -X_{11}(z)z^{-k}. \tag{2.12}$$

Taking the inverse z transform of (2.9)–(2.12) and combining the results with (2.5)–(2.8), we obtain

$$\hat{s}_{0k}(n+1) = \hat{s}_{0k}(n) + 2\mu[\alpha_0 E(e_0(n)x_{00}(n-k)) + \alpha_1 E(e_1(n)x_{10}(n-k))] \tag{2.13}$$

$$\hat{s}_{1k}(n+1) = \hat{s}_{1k}(n) + 2\mu[\alpha_0 E(e_0(n)x_{01}(n-k)) + \alpha_1 E(e_1(n)x_{11}(n-k))] \tag{2.14}$$

for $k = 0, 1, \cdots (L/2) - 1$.

Now, we replace the true gradient by the instantaneous gradient and express the update equations as

$$\hat{s}_{0k}(n+1) = \hat{s}_{0k}(n) + 2\mu[\alpha_0 e_0(n)x_{00}(n-k) + \alpha_1 e_1(n)x_{10}(n-k)] \tag{2.15}$$

$$\hat{s}_{1k}(n+1) = \hat{s}_{1k}(n) + 2\mu[\alpha_0 e_0(n)x_{01}(n-k) + \alpha_1 e_1(n)x_{11}(n-k)]. \tag{2.16}$$

These are the LMS adaptation equations for the coefficients of $\hat{S}_0(z)$ and $\hat{S}_1(z)$. It is to be noted that the filters $\hat{S}_0(z)$ and $\hat{S}_1(z)$ in the two subbands are constrained to be the same.

C. Asymptotic Convergence Analysis

We will now study the convergence of the coefficient error vector with the above adaptation rule.

We decompose $S(z)$ as

$$S(z) = S_0(z^2) + z^{-1}S_1(z^2) \tag{2.17}$$

and define the coefficient error vector at the nth iteration as

$$\boldsymbol{v}_0(n) = \boldsymbol{s}_0 - \hat{\boldsymbol{s}}_0(n) \tag{2.18}$$

$$\boldsymbol{v}_1(n) = \boldsymbol{s}_1 - \hat{\boldsymbol{s}}_1(n) \tag{2.19}$$

where $\boldsymbol{s}_0$ and $\boldsymbol{s}_1$ denote the coefficient vectors of $S_0(z)$ and $S_1(z)$, respectively, and $\hat{\boldsymbol{s}}_0(n)$ and $\hat{\boldsymbol{s}}_1(n)$ denote the coefficient vectors of $\hat{S}_0(z)$ and $\hat{S}_1(z)$, respectively, at the nth iteration. Using the input-output relation of the decimator, we can write the z transform of $y_0(n)$ (see Fig. 4) as

$$Y_0(z) = \tfrac{1}{2}[H_0(z^{1/2})Y(z^{1/2})S(z^{1/2}) + H_0(-z^{1/2})Y(-z^{1/2})S(-z^{1/2})] \tag{2.20}$$

which in view of (2.17) can be expressed as

$$Y_0(z) = \frac{S_0(z)}{2}[H_0(z^{1/2})Y(z^{1/2}) + H_0(-z^{1/2})Y(-z^{1/2})] + \frac{S_1(z)}{2}[H_0(z^{1/2})Y(z^{1/2})z^{-(1/2)} + H_0(-z^{1/2})Y(-z^{1/2})(-z)^{-(1/2)}]. \tag{2.21}$$

Noting that

$$X_{00}(z) = \tfrac{1}{2}[H_0(z^{1/2})Y(z^{1/2}) + H_0(-z^{1/2})Y(-z^{1/2})] \tag{2.22}$$

and

$$X_{01}(z) = \tfrac{1}{2}[H_0(z^{1/2})Y(z^{1/2})z^{-(1/2)} + H_0(-z^{1/2})Y(-z^{1/2})(-z)^{-(1/2)}] \tag{2.23}$$

(2.21) can be simplified as

$$Y_0(z) = S_0(z)X_{00}(z) + S_1(z)X_{01}(z). \tag{2.24}$$

Similarly, we obtain

$$Y_1(z) = S_0(z)X_{10}(z) + S_1(z)X_{11}(z). \tag{2.25}$$

Combining (2.24) and (2.25) with (2.2) and (2.3), we get

$$E_0(z) = X_{00}(z)[S_0(z) - \hat{S}_0(z)] + X_{01}(z)[S_1(z) - \hat{S}_1(z)] \tag{2.26}$$

$$E_1(z) = X_{10}(z)[S_0(z) - \hat{S}_0(z)] + X_{11}(z)[S_1(z) - \hat{S}_1(z)]. \tag{2.27}$$

Taking the inverse z transform of (2.26) and (2.27) and expressing the results in vector form, we have

$$e_0(n) = \boldsymbol{x}_{00}^T(n)\boldsymbol{v}_0(n) + \boldsymbol{x}_{01}^T(n)\boldsymbol{v}_1(n) \tag{2.28}$$

$$e_1(n) = \boldsymbol{x}_{10}^T(n)\boldsymbol{v}_0(n) + \boldsymbol{x}_{11}^T(n)\boldsymbol{v}_1(n) \tag{2.29}$$

where $\boldsymbol{x}_{lk}^T(n) = [x_{lk}(n)\ x_{lk}(n-1)\ \cdots\ x_{lk}(n-(L/2)+1)], l, k = 0, 1$.

Using (2.28) and (2.29) in (2.15) and (2.16) and the definitions of (2.18) and (2.19), the recursive relations for the coefficient error vector can be obtained as

$$\begin{aligned}\boldsymbol{v}_0(n+1) = \boldsymbol{v}_0(n) &- 2\mu\alpha_0\boldsymbol{x}_{00}(n)\boldsymbol{x}_{00}^T(n)\boldsymbol{v}_0(n) \\ &- 2\mu\alpha_0\boldsymbol{x}_{00}(n)\boldsymbol{x}_{01}^T(n)\boldsymbol{v}_1(n) \\ &- 2\mu\alpha_1\boldsymbol{x}_{10}(n)\boldsymbol{x}_{10}^T(n)\boldsymbol{v}_0(n) \\ &- 2\mu\alpha_1\boldsymbol{x}_{10}(n)\boldsymbol{x}_{11}^T(n)\boldsymbol{v}_1(n)\end{aligned} \tag{2.30}$$

$$\begin{aligned}\boldsymbol{v}_1(n+1) = &\boldsymbol{v}_1(n) - 2\mu\alpha_0\boldsymbol{x}_{01}(n)\boldsymbol{x}_{00}^T(n)\boldsymbol{v}_0(n)\\ &- 2\mu\alpha_0\boldsymbol{x}_{01}(n)\boldsymbol{x}_{01}^T(n)\boldsymbol{v}_1(n)\\ &- 2\mu\alpha_1\boldsymbol{x}_{11}(n)\boldsymbol{x}_{10}^T(n)\boldsymbol{v}_0(n)\\ &- 2\mu\alpha_1\boldsymbol{x}_{11}(n)\boldsymbol{x}_{11}^T(n)\boldsymbol{v}_1(n). \qquad (2.31)\end{aligned}$$

Expressing (2.30) and (2.31) in vector form, we have

$$\begin{aligned}\begin{bmatrix}\boldsymbol{v}_0(n+1)\\ \boldsymbol{v}_1(n+1)\end{bmatrix} = &\begin{bmatrix}\boldsymbol{v}_0(n)\\ \boldsymbol{v}_1(n)\end{bmatrix}\\ &- 2\mu[\alpha_0\boldsymbol{A}_0(n) + \alpha_1\boldsymbol{A}_1(n)]\begin{bmatrix}\boldsymbol{v}_0(n)\\ \boldsymbol{v}_1(n)\end{bmatrix}\end{aligned} \qquad (2.32)$$

where

$$\boldsymbol{A}_0(n) = \begin{bmatrix}\boldsymbol{x}_{00}(n)\boldsymbol{x}_{00}^T(n) & \boldsymbol{x}_{00}(n)\boldsymbol{x}_{01}^T(n)\\ \boldsymbol{x}_{01}(n)\boldsymbol{x}_{00}^T(n) & \boldsymbol{x}_{01}(n)\boldsymbol{x}_{01}^T(n)\end{bmatrix} \qquad (2.33)$$

$$\boldsymbol{A}_1(n) = \begin{bmatrix}\boldsymbol{x}_{10}(n)\boldsymbol{x}_{10}^T(n) & \boldsymbol{x}_{10}(n)\boldsymbol{x}_{11}^T(n)\\ \boldsymbol{x}_{11}(n)\boldsymbol{x}_{10}^T(n) & \boldsymbol{x}_{11}(n)\boldsymbol{x}_{11}^T(n)\end{bmatrix}. \qquad (2.34)$$

We now consider the mean behavior of the coefficient error vector, as is usually done in the LMS algorithm analysis [8]. Taking expectation on both sides of (2.32), we have

$$\begin{aligned}E\begin{bmatrix}\boldsymbol{v}_0(n+1)\\ \boldsymbol{v}_1(n+1)\end{bmatrix} = &E\begin{bmatrix}\boldsymbol{v}_0(n)\\ \boldsymbol{v}_1(n)\end{bmatrix}\\ &- 2\mu E[\alpha_0\boldsymbol{A}_0(n) + \alpha_1\boldsymbol{A}_1(n)]E\begin{bmatrix}\boldsymbol{v}_0(n)\\ \boldsymbol{v}_1(n)\end{bmatrix}\end{aligned} \qquad (2.35)$$

where we have implicitly assumed the independence of the two terms appearing on the right-hand side of (2.32), which is usually made in such analysis. Equation (2.35) can now be expressed as

$$\begin{bmatrix}E(\boldsymbol{v}_0(n+1))\\ E(\boldsymbol{v}_1(n+1))\end{bmatrix} = [\boldsymbol{I}_L - 2\mu\boldsymbol{\Phi}]\begin{bmatrix}E(\boldsymbol{v}_0(n))\\ E(\boldsymbol{v}_1(n))\end{bmatrix} \qquad (2.36)$$

where

$$\boldsymbol{\Phi} = \alpha_0 E[\boldsymbol{A}_0(n)] + \alpha_1 E[\boldsymbol{A}_1(n)] \qquad (2.37)$$

and $\boldsymbol{I}_L$ denotes the identity matrix of order L.

It can be shown [10] that $\boldsymbol{\Phi}$ is positive definite. Let the ordered eigenvalues of $\boldsymbol{\Phi}$ be denoted as

$$\lambda_1 \le \lambda_2 \le \cdots \le \lambda_L. \qquad (2.38)$$

We can then show [8] that the mean coefficient error vector converges to zero asymptotically if

$$0 < \mu < \frac{1}{\lambda_L}. \qquad (2.39)$$

The convergence rate, however, depends on the eigenvalue spread. We show in later sections that our formulation (cost function) brings down this eigenvalue spread, forcing it close to unity with increasing value of M.

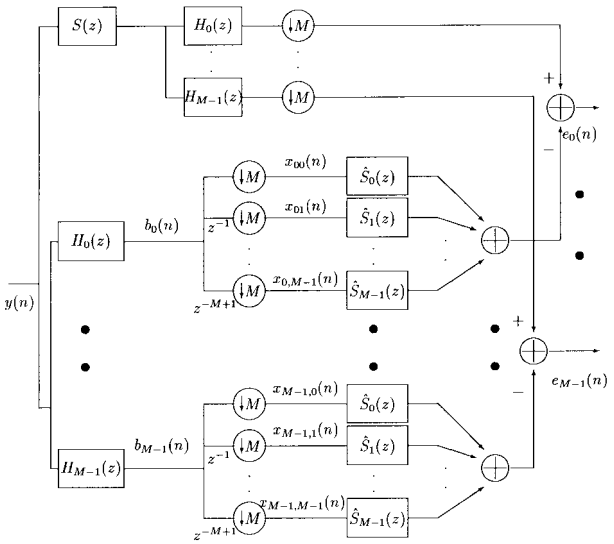

Fig. 5. SAF for M-band case.

III. Extension to M-Band Case

Here, we decompose the adaptive filter $\hat{S}(z)$ into M polyphase components

$$\hat{S}(z) = \hat{S}_0(z^M) + z^{-1}\hat{S}_1(z^M) + \cdots + z^{-M+1}\hat{S}_{M-1}(z^M). \qquad (3.1)$$

Each of the polyphase components can be moved across the decimator. The SAF structure for this case is shown in Fig. 5.

As seen from the figure, there are M filters, each of length L/M, at the output of each analysis filter. These filters have to be adapted. The cost function in this case is the extension of (2.4)

$$J(n) = E[\alpha_0 e_0^2(n) + \alpha_1 e_1^2(n) + \cdots + \alpha_{M-1}e_{M-1}^2(n)] \qquad (3.2)$$

where the constants $\alpha_0, \alpha_1, \cdots, \alpha_{M-1}$ are inversely proportional to the powers of $b_0(n), b_1(n), \cdots, b_{M-1}(n)$, respectively. This is, again, a weighted cost function, with more weight given to the error corresponding to the subband of lower signal power. Following the steps as in the two-band case, we can obtain the adaptation equations for the filter coefficients as

$$\begin{aligned}\hat{s}_{ki}(n+1) = &\hat{s}_{ki}(n) + 2\mu\sum_{l=0}^{M-1}\alpha_l e_l(n)x_{lk}(n-i)\\ &k = 0, 1, \cdots, (M-1)\\ &i = 0, 1, \cdots, \left(\frac{L}{M} - 1\right). \qquad (3.3)\end{aligned}$$

Extending the analysis of the two-band case, we have

$$E\begin{bmatrix}\boldsymbol{v}_0(n+1)\\ \boldsymbol{v}_1(n+1)\\ \vdots\\ \boldsymbol{v}_{M-1}(n+1)\end{bmatrix} = [\boldsymbol{I}_L - 2\mu\boldsymbol{\Phi}]E\begin{bmatrix}\boldsymbol{v}_0(n)\\ \boldsymbol{v}_1(n)\\ \vdots\\ \boldsymbol{v}_{M-1}(n)\end{bmatrix} \qquad (3.4)$$

where

$$\boldsymbol{\Phi} = \alpha_0\boldsymbol{\Phi}_0 + \alpha_1\boldsymbol{\Phi}_1 + \cdots + \alpha_{M-1}\boldsymbol{\Phi}_{M-1} \qquad (3.5)$$

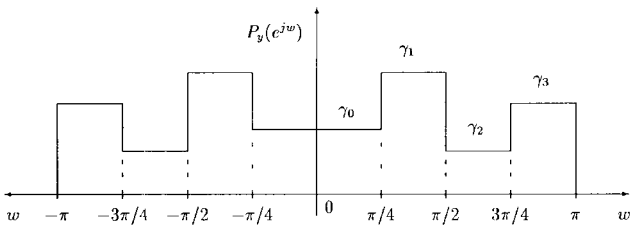

Fig. 6. Sample spectrum of $y(n)$.

with

$$\boldsymbol{\Phi}_k = E\left(\begin{bmatrix} \boldsymbol{x}_{k0}(n) \\ \boldsymbol{x}_{k1}(n) \\ \vdots \\ \boldsymbol{x}_{k,M-1}(n) \end{bmatrix} [\boldsymbol{x}_{k0}^T(n)\, \boldsymbol{x}_{k1}^T(n)\, \cdots\, \boldsymbol{x}_{k,M-1}^T(n)]\right) \quad k = 0, 1, \cdots, (M-1). \tag{3.6}$$

As in the two-band case, the matrix $\boldsymbol{\Phi}$ is positive definite. The mean coefficient error vector converges to zero asymptotically if the step size is chosen according to $0 < \mu < (1/\lambda_{\max})$, where $\lambda_{\max}$ is the maximum eigenvalue of $\boldsymbol{\Phi}$.

IV. Convergence Performance and Computational Complexity

In this section, we bring out how our formulation forces $\boldsymbol{\Phi}$ close to a scalar multiple of an identity matrix, i.e., $||\boldsymbol{\Phi} - \beta \boldsymbol{I}||_F$ is close to zero, where $||\boldsymbol{A}||_F$ denotes the Frobenius norm of $\boldsymbol{A}$ and β is a scalar constant, thereby leading to improved rate of convergence of the adaptation algorithm. We do this by taking a sample spectrum for the input signal and considering ideal filters for the analysis bank. We also discuss the computational complexity of the proposed scheme.

A. Structure of $\boldsymbol{\Phi}$

For the purpose of clarity, we consider the four-band case with $L = 8$ (length of $\hat{S}(z) = 8$), and hence, the corresponding vectors $\{\boldsymbol{x}_{kl}(n)\}$ will be of length 2. We assume that the power spectrum of $y(n)$, $P_y(e^{jw})$, is piecewise flat, as shown in Fig. 6.

Recall that

$$\boldsymbol{\Phi} = \sum_{k=0}^{3} \alpha_k \boldsymbol{\Phi}_k$$

where $\boldsymbol{\Phi}_k$ is the autocorrelation matrix given in (3.6). For $M = 4$, $\boldsymbol{\Phi}_k$ is given by

$$\boldsymbol{\Phi}_k = E\left(\begin{bmatrix} \boldsymbol{x}_{k0}(n) \\ \boldsymbol{x}_{k1}(n) \\ \boldsymbol{x}_{k2}(n) \\ \boldsymbol{x}_{k3}(n) \end{bmatrix} [\boldsymbol{x}_{k0}^T(n)\, \boldsymbol{x}_{k1}^T(n)\, \boldsymbol{x}_{k2}^T(n)\, \boldsymbol{x}_{k3}^T(n)]\right) \tag{4.1}$$

with

$$\boldsymbol{x}_{kl}(n) = [b_k(l+4n)\, b_k(l+4n+4)]^T. \tag{4.2}$$

Thus, we have (4.3), shown at the bottom of the page, where

$$r_k(m) = E[b_k(n) b_k(n+m)]. \tag{4.4}$$

We now assume the analysis filters $H_0(e^{jw})$, $H_1(e^{jw})$, $H_2(e^{jw})$, and $H_3(e^{jw})$ to be ideal with bandwidth of $\pi/4$. All these filters can be obtained from a prototype lowpass ideal filter of passband $-\pi/8$ to $\pi/8$, which is denoted by $H(e^{jw})$, by cosine modulation. We can thus express

$$H_k(e^{jw}) = H(e^{j(w-w_k)}) + H(e^{j(w+w_k)}) \tag{4.5}$$

where $w_k = (2k+1)(\pi/8), k = 0, 1, 2, 3$.

Now, $P_y(e^{jw})$ can be written as

$$P_y(e^{jw}) = \sum_{k=0}^{3} \gamma_k (P(e^{j(w-w_k)}) + P(e^{j(w+w_k)})) \tag{4.6}$$

where $P(e^{jw})$ is unity between $-\pi/8$ and $\pi/8$ and zero elsewhere. The power spectrum of $b_k(n)$, which is denoted by $P_k(e^{jw})$, is then given by

$$P_k(e^{jw}) = P_y(e^{jw}) |H_k(e^{jw})|^2 \tag{4.7}$$

which, in view of (4.5), can be expressed as

$$P_k(e^{jw}) = P_y(e^{jw}) |H(e^{j(w-w_k)})|^2 + P_y(e^{jw}) |H(e^{j(w+w_k)})|^2. \tag{4.8}$$

From (4.6) and the fact that $H(e^{j(w \pm w_k)})$ and $P(e^{j(w \pm w_k)})$ have the same characteristics, (4.8) simplifies to

$$P_k(e^{jw})) = \gamma_k [P(e^{j(w-w_k)}) + P(e^{j(w+w_k)})]. \tag{4.9}$$

Let $p(n)$ be the inverse Fourier transform of $P(e^{jw})$. We can then write

$$r_k(n) = 2\gamma_k p(n) \cos(w_k n), \qquad k = 0, 1, 2, 3. \tag{4.10}$$

$$\boldsymbol{\Phi}_k = \begin{bmatrix} r_k(0) & r_k(4) & r_k(1) & r_k(5) & r_k(2) & r_k(6) & r_k(3) & r_k(7) \\ r_k(4) & r_k(0) & r_k(3) & r_k(1) & r_k(2) & r_k(2) & r_k(1) & r_k(3) \\ r_k(1) & r_k(3) & r_k(0) & r_k(4) & r_k(1) & r_k(5) & r_k(2) & r_k(6) \\ \vdots & \vdots & \vdots & \vdots & \vdots & \vdots & \vdots & \vdots \\ \vdots & \vdots & \vdots & \vdots & \vdots & \vdots & \vdots & \vdots \\ \vdots & \vdots & \vdots & \vdots & \vdots & \vdots & \vdots & \vdots \\ \vdots & \vdots & \vdots & \vdots & \vdots & \vdots & \vdots & \vdots \\ r_k(7) & r_k(3) & r_k(6) & r_k(2) & r_k(5) & r_k(1) & r_k(4) & r_k(0) \end{bmatrix} \tag{4.3}$$

Recall that α_k, which is the weight applied to $e_k^2(n)$ in (3.2), is c/γ_k, where c is a proportionality constant. Let

$$q(n) = \sum_{k=0}^{3} \alpha_k r_k(n). \tag{4.11}$$

Then, from (3.5), (4.3), and (4.11), we can express $\boldsymbol{\Phi}$ as

$$\boldsymbol{\Phi} = \begin{bmatrix} q(0) & q(4) & q(1) & q(5) & q(2) & q(6) & q(3) & q(7) \\ q(4) & q(0) & q(3) & q(1) & q(2) & q(2) & q(1) & q(3) \\ q(1) & q(3) & q(0) & q(4) & q(1) & q(5) & q(2) & q(6) \\ \vdots & \vdots & \vdots & \vdots & \vdots & \vdots & \vdots & \vdots \\ \vdots & \vdots & \vdots & \vdots & \vdots & \vdots & \vdots & \vdots \\ \vdots & \vdots & \vdots & \vdots & \vdots & \vdots & \vdots & \vdots \\ \vdots & \vdots & \vdots & \vdots & \vdots & \vdots & \vdots & \vdots \\ \vdots & \vdots & \vdots & \vdots & \vdots & \vdots & \vdots & \vdots \\ q(7) & q(3) & q(6) & q(2) & q(5) & q(1) & q(4) & q(0) \end{bmatrix}. \tag{4.12}$$

Combining (4.10) and (4.11) and substituting c/γ_k for α_k, we get

$$q(n) = 2cp(n) \sum_{k=0}^{3} \cos(w_k n). \tag{4.13}$$

Since $w_k = (2k+1)(\pi/8), k = 0, 1, 2, 3$, it is easy to show that $\Sigma_{k=0}^{3} \cos(w_k n)$ is nonzero only for $n = 8m, m = \cdots, -2, -1, 0, 1, 2, \cdots$. Now, because of the nature of $P(e^{jw})$, its inverse Fourier transform $p(n)$ is a sinc function with zeros at $n = 8m$ for $m = \cdots, -2, -1, 1, 2, \cdots$. Therefore, $q(n)$ is nonzero only for $n = 0$. Thus, the matrix $\boldsymbol{\Phi}$ is diagonal with identical diagonal elements. That is, $\boldsymbol{\Phi} = \beta \boldsymbol{I}$, where $\beta = q(0)$. This means that the eigenvalue spread of $\boldsymbol{\Phi}$ is unity. It is well known that the convergence rate of the LMS algorithm is fastest under this condition.

In practice, however, i) analysis filters have finite transition bandwidth and finite attenuation in the stopband, and ii) the power spectrum of the input signal may not be piece-wise flat. In such a case, $\boldsymbol{\Phi}$ will not be a scalar multiple of the identity matrix. However, as we increase the number of bands M, it tends to a scalar multiple of $\boldsymbol{I}$, provided the analysis filters are of good quality (but not necessarily ideal). The simulation results given in the next section corroborate this fact.

B. Computational Complexity

We will now discuss the computational complexity of the proposed approach. For the convolutions of subband signals with the polyphase components of $\hat{S}(z)$, the computations are carried out once for every M input samples. Thus, for every M input samples, we perform M^2 convolutions of length $(L/M), M$ additions, each involving M elements and M subtractions to get M subband error signals. This comes to (LM) multiplications and (LM) additions for every M input samples.

In the adaptation, we need to calculate $\alpha_0, \alpha_1, \cdots, \alpha_{M-1}$. Since we compute them only once, we do not consider the computations required for their calculations. As the filter coefficients are adapted once every M input samples, the adaptation algorithm requires $(M+ML)$ multiplications and (ML) additions for every M input samples. In addition to the above computations, we have the complexity of the filter banks. There are two analysis banks and one synthesis bank. With efficient implementations, the computations required by these banks can be made considerably low (these computations, however, depend on the quality of the analysis filters, and they may become more significant as the filters approach the ideal case). Thus, for every M input samples, the total number of computations required are $(2L+1)M$ multiplications and $2LM$ additions.

Now, the computations required in the fullband filter case are as follows. For the convolution of the input with the estimated impulse response, which is of length L, we need L multiplications/input sample and $(L-1)$ additions/input sample. In the adaptation, we need $(L+1)$ multiplications/input sample, L additions/input sample, and one subtraction/input sample to get the error signal. Thus, the fullband adaptive filter requires $(2L+1)$ multiplications and $(2L)$ additions/input sample. Thus, the computational complexity of the proposed SAF is nearly same as that of fullband adaptive filter.

V. Simulation Results

In this section, we study the convergence performance of the SAF using simulations. The input signal is a first-order autoregressive (AR) process with white Gaussian noise as the driving input. That is, $y(n)$ is modeled as $y(n) = \rho y(n-1) + u(n)$, where $u(n)$ is a white Gaussian noise sequence. In our simulations, we fixed ρ at 0.9. The system noise is a white Gaussian noise sequence that is independent of the $u(n)$.

We considered two sets of simulations. In the first set, the length of $S(z)$ [and of $\hat{S}(z)$] was kept at 80, i.e., $L = 80$, whereas in the second set, this was increased to 1000. In each case, the coefficients of the filter $S(z)$ were chosen randomly. The normalized coefficient error vector norm and mean square error (in decibels) at time n, which is defined as

$$10 \log_{10} \frac{\boldsymbol{v}^T(n)\boldsymbol{v}(n)}{\boldsymbol{s}^T\boldsymbol{s}}$$

and $10 \log_{10} e^2(n)$, respectively, where $\boldsymbol{v}^T(n) = [\boldsymbol{v}_0^T(n)\boldsymbol{v}_1^T(n)\cdots\boldsymbol{v}_{M-1}^T(n)]$, and $\boldsymbol{s}^T = [\boldsymbol{s}_0^T\boldsymbol{s}_1^T\cdots\boldsymbol{s}_{M-1}^T]$, are used to depict the convergence performance. We normalized the input $y(n)$ such that the variance of the resulting sequence at the output of $S(z)$ was unity. In each case, i.e., for $L = 80$ and 1000, we considered two levels of system noise: no noise and -30 dB noise. In the simulations, we discarded the first 2000 samples of $y(n)$ so that the actual AR sequence used was nearly stationary. The coefficients $\{\alpha_k\}$ were computed as the inverse of the powers of $\{b_k(n)\}$ estimated from the overall samples used in the adaptation. The selection of the step size μ was made as follows.

In the fullband case, we used a normalized LMS algorithm, whereas in the sub-band case, the algorithm as given by (3.3) was implemented, initializing the coefficients of $\hat{S}(z)$ to zero in each case. The best possible value for μ (best in the sense that it yields fastest convergence with the converged value as close to the noise level as possible) was found by trial and error. Since the value of μ has to satisfy the condition

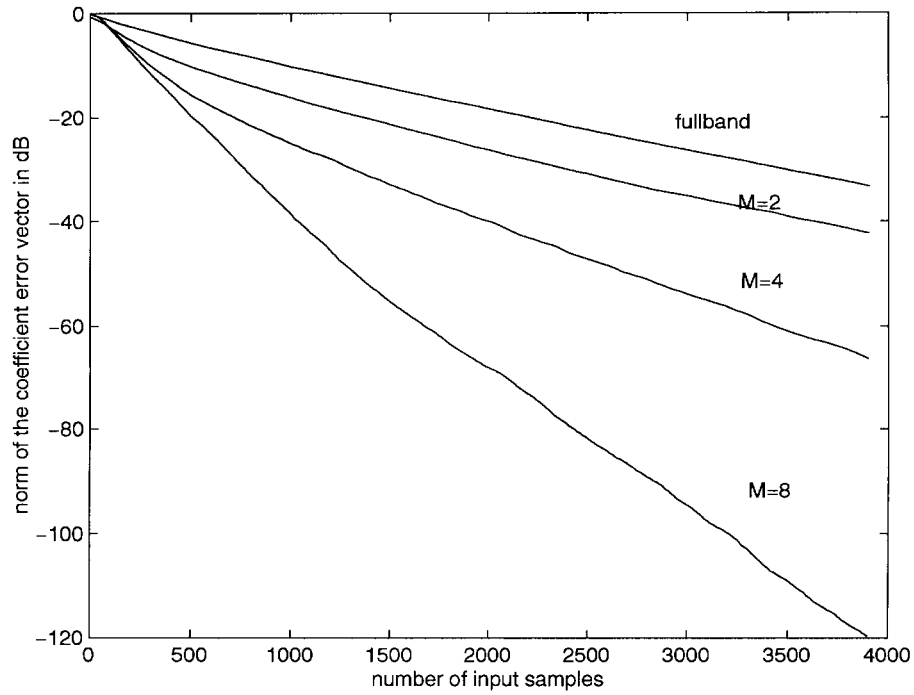

Fig. 7. Convergence performance of the SAF for different values of M with system noise absent (filter length $L = 80$ and step sizes (μ values) are 0.675, 0.0038, 0.0033, and 0.0028 for fullband, $M = 2, M = 4$, and $M = 8$, respectively).

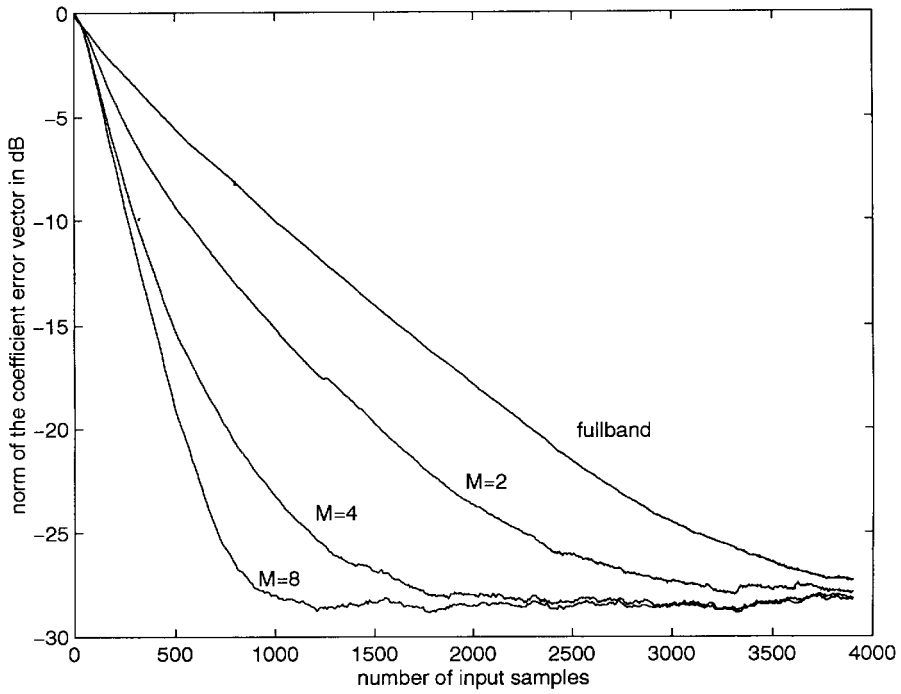

Fig. 8. Convergence performance of the SAF for different values of M with system noise level of -30 dB (filter length $L = 80$ and step sizes (μ values) are 0.675, 0.0038, 0.0033, and 0.0028 for fullband, $M = 2, M = 4$, and $M = 8$, respectively).

$0 < \mu < 1/\lambda_{\max}$, where $\lambda_{\max}$ is the maximum eigenvalue of $\boldsymbol{\Phi}$ and $\boldsymbol{\Phi}$ does not depend on the system noise level [see (3.5)], the best value for μ was found for the noise level of -30 dB, and the same was used in the no-noise case. Note that the value of μ so found depends on the value of M. The norm and mean square error (MSE) curves were averaged over 25 Monte Carlo runs.

Recall that the adaptations are carried out once for every M input samples in the SAF case. This means that for $M = 2$, the time elapsed for k adaptations spans $2k$ input samples whereas for $M = 8$, it spans $8k$ input samples. We therefore present the plots for different values of M as a function of the number of input samples. Further, the delays introduced by the analysis bank alone and that introduced by the cascade

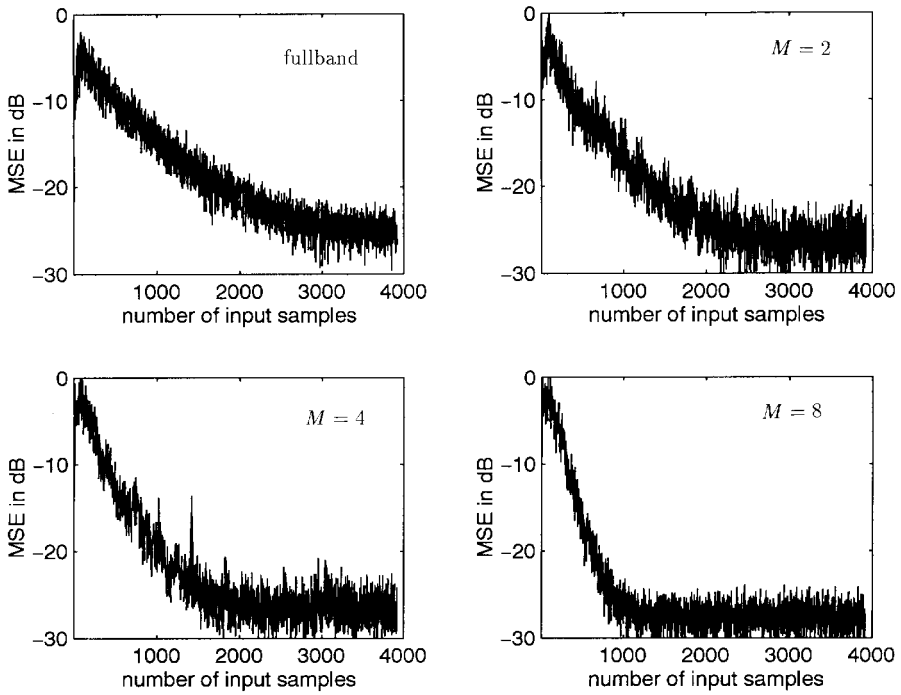

Fig. 9. MSE curves, depicting the convergence performance of the SAF, with system noise level of -30 dB (filter length $L = 80$ and step sizes (μ values) are 0.675, 0.0038, 0.0033, and 0.0028 for fullband, $M = 2, M = 4$, and $M = 8$, respectively).

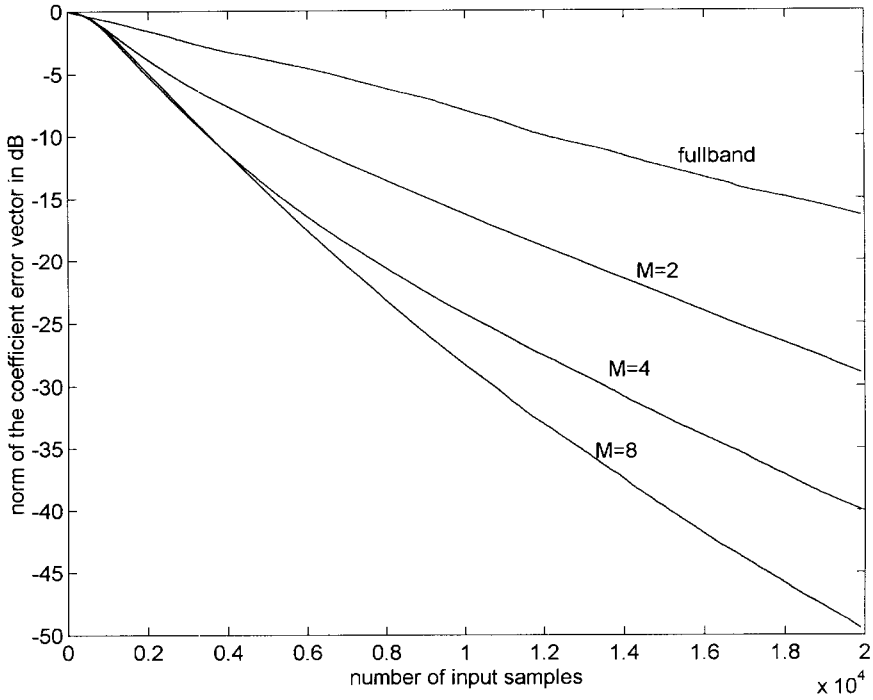

Fig. 10. Convergence performance of the SAF for different values of M with system noise absent (filter length $L = 1000$ and step sizes (μ values) are 0.50, 0.0005, 0.000 35, and 0.000 25 for fullband, $M = 2, M = 4$, and $M = 8$, respectively).

of analysis and synthesis banks are taken into account while plotting the coefficient error vector norm and MSE curves, respectively. That is, the norm and MSE curves are plotted without the effect of the filter bank delay. We may point out here that for both cases of L (i.e., $L = 80$ and $L = 1000$), the lengths of the analysis filters (as well as the synthesis filters) were increased with M so that the ratio of the transition band to the passband was maintained nearly the same for all values of M. In particular, we used filters (analysis and synthesis) with lengths 20, 40, and 80 for $M = 2, 4$, and 8, respectively.

Figs. 7–9 correspond to the first set, i.e., for $L = 80$. The plots of Fig. 7 (for the no-noise case) clearly show that the convergence rate goes up with M. Since the system noise is zero, the converged value will be (theoretically speaking) $-\infty$.

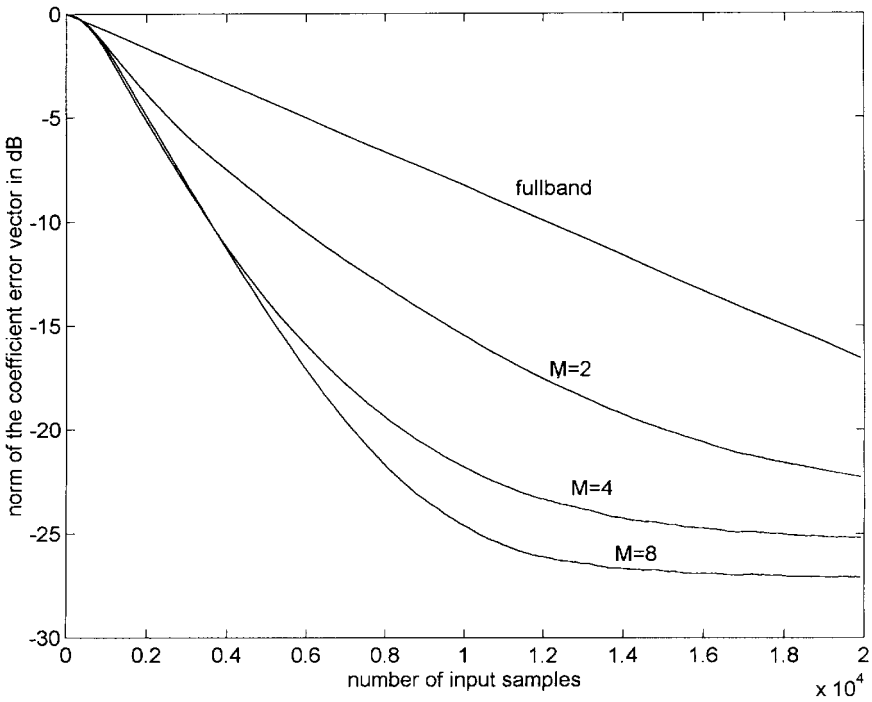

Fig. 11. Convergence performance of the SAF for different values of M with system noise level of -30 dB (filter length $L = 1000$ and step sizes (μ values) are 0.50, 0.0005, 0.000 35, and 0.000 25 for fullband, $M = 2, M = 4$, and $M = 8$, respectively).

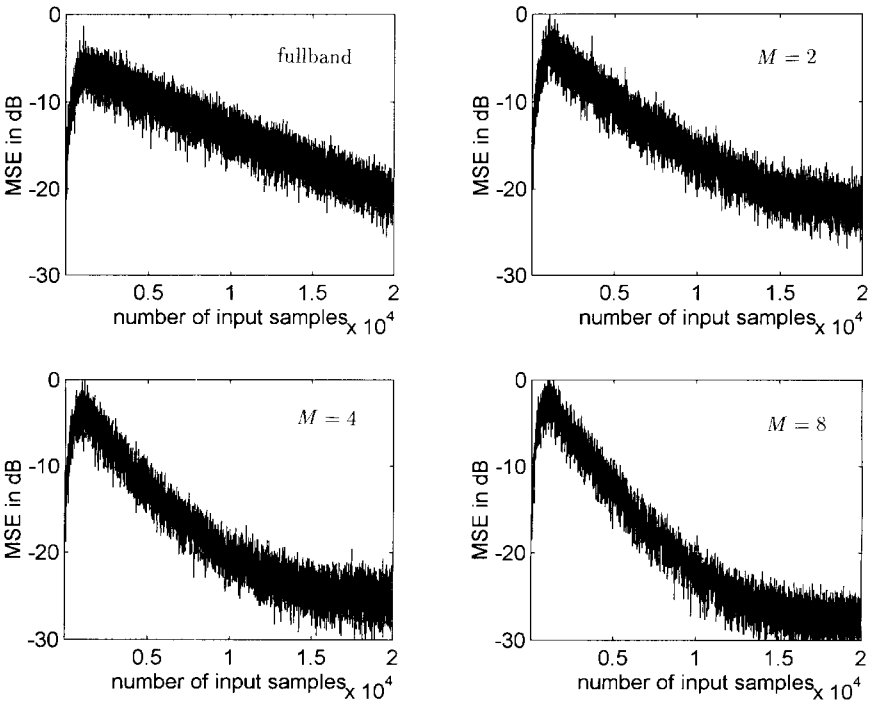

Fig. 12. MSE curves depicting the convergence performance of the SAF with system noise level of -30 dB (filter length $L = 1000$ and step sizes (μ values) are 0.50, 0.0005, 0.000 35, and 0.000 25 for fullband, $M = 2, M = 4$, and $M = 8$, respectively).

The curves of Fig. 8 (which correspond to the system noise level of -30 dB), on the other hand, show that the coefficient error vector norm converges to about 1.5 dB above the system noise level in the fullband and subband cases, whereas the rate at which this happens goes up with increasing value of M. The difference between the converged value and the system noise level is mainly because of the misadjustment noise. Fig. 9 gives the MSE curves for -30 dB noise. Note, once again, that the converged value is slightly above the system noise level and that the convergence rate increases with M.

Figs. 10–12 correspond to the second set, i.e., for $L = 1000$. In this case, we used 20 000 data samples to study the convergence. Note from the plots that the convergence rate goes up with M. The converged value is about 3 dB higher

TABLE I
EIGENVALUE SPREAD OF THE $\boldsymbol{\Phi}$ MATRIX

filter length	fullband	2-band	4-band	8-band
L=80	381.5	163.6	34.9	7.1
L=1000	1302.3	973.1	134.8	29.0

than the noise level (see Figs. 11 and 12), which is more than the value in Figs. 8 and 9. This is because the misadjustment noise level is usually higher when the filter length is larger. In the present case, the filter length is around 12 times that of the filter used in the simulations corresponding to Figs. 7–9. We may also point out here that the converged values (see Fig. 11) may appear to be different for different values of M. However, this difference will come down if the adaptation is continued further, and eventually, the difference will become negligible.

Choosing a sample input spectrum that is piecewise flat and assuming ideal analysis filters, we have shown in Section IV how our formulation forces $\boldsymbol{\Phi}$ to $\beta \boldsymbol{I}$. With overlapping analysis filters and an input signal whose spectrum is not piece-wise flat, we conjectured that $\boldsymbol{\Phi}$ tends to a scalar multiple of the identity matrix as M is increased. To substantiate this, we computed the eigenvalue spread (which is measured as the ratio of the maximum to the minimum eigenvalue) of the $\boldsymbol{\Phi}$ matrix for different values of M and for different filter lengths and presented the results in Table I.

Note that the eigenvalue spread comes down by a factor of 55 in the case of $L = 80$ and 45 for $L = 1000$ as M is increased to 8. This reduction in the eigenvalue spread results in the increased convergence rate with M.

VI. CONCLUSIONS

A new structure and a new formulation for the SAF are presented in this paper. With the weighted cost function, the convergence rate of the SAF improves considerably with increasing value of M. The cross filters are totally avoided in the structure, and the adaptive filters in the subbands are independent of the analysis and synthesis filters. Any perfect reconstruction system with "good" filter characteristics can be used in our approach. The overall computational complexity is nearly the same as that of fullband adaptive filter. The simulation results support the theoretical predictions.

ACKNOWLEDGMENT

The authors wish to thank the reviewers for their critical and helpful comments, which improved the quality of the paper.

REFERENCES

[1] Y. Itoh *et al.*, "An acoustic echo canceler for teleconference," in *Proc. IEEE ICC*, 1985, pp. 1498–1502.
[2] A. Gilloire, "Experiments with subband acoustic echo cancelers for teleconferencing," in *Proc. IEEE ICASSP*, 1987, pp. 2141–2144.
[3] J. Chen, H. Bes, J. Vandewalle, and P. Janssens, "A new structure for subband acoustic echo canceler," in *Proc. IEEE ICASSP*, 1988, pp. 2574–2577.
[4] M. R. Asharif, F. Amano, S. Unagami, and K. Morano, "Acoustic echo canceler based on frequency bin adaptive filtering (FBAF)," *Proc. IEEE GLOBECOM*, 1987, pp. 49.2.1–49.2.5.
[5] S. J. Orfanidis, *Optimum Signal Processing: An Introduction*. New York: Macmillan, 1985.
[6] S. T. Alexander, *Adaptive Signal Processing: Theory and Applications*. New York: Springer-Verlag, 1986.
[7] D. G. Messerschmitt, "Echo cancellation in speech and data transmission," *IEEE J. Select. Areas. Commun.*, vol. SAC-2, Mar. 1984.
[8] B. Widrow *et al.*, "Adaptive noise cancellation: Principles and applications," *Proc. IEEE*, vol. 63, no. 12, Dec. 1975.
[9] W. Kellermann, "Analysis and design of multirate systems for cancellation of acoustical echoes," *Proc. IEEE ICASSP*, 1988, pp. 2570–2573.
[10] A. Gilloire and M. Vetterli, "Adaptive filtering in subbands with critical sampling: Analysis, experiments and application to acoustic echo cancellation," *IEEE Trans. Signal Processing*, vol. 40, pp. 1862–1875, Aug. 1992.
[11] H. Yasukawa, S. Shimada, and I. Furukawa, "Acoustic echo canceler with high speech quality," *Proc. IEEE ICASSP*, 1987, pp. 2125–2128.
[12] P. P. Vaidyanathan, *Multirate Systems and Filter Banks*. Englewood Cliffs, NJ: Prentice-Hall, 1993.

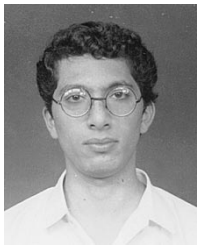

S. Sandeep Pradhan was born in India on August 14, 1972. He received the M.E. degree in electrical communication engineering from the Indian Institute of Science (IISc), Bangalore, in January 1996.

He was a Project Associate at IISc from January 1996 to July 1996. Presently, he is a Graduate Research Assistant at the Beckman Institute and Department of Electrical and Computer Engineering, University of Illinois, Urbana. His research interests include information theory, coding theory, quantization, and multirate signal processing.

V. U. Reddy (SM'82–F'99) received the B.E. and M.Tech. degrees in electronics and communication engineering from the Osmania University, Hyderabad, India, and the Indian Insitute of Tecnology (IIT), Kharagpur, in 1962 and 1963, respectively, and the Ph.D. degree in electrical engineering from the University of Missouri, Columbia, in 1971.

He was an Assistant Professor at IIT, Madras, from 1972 to 1976, and a Professor at IIT, Kharagpur, from 1976 to 1979. From 1979 to 1982, he was a Visiting Professor at the Department of Electrical Engineering, Stanford University, Stanford, CA. On an invitation from the Osmania University to head a major project funded by the Department of Electronics, Government of India, he joined the University in April 1982 and founded the Research and Training Unit for Navigational Electronics (which is now a permanent centre of the University). Since April 1988, he has been with the Indian Institute of Science, as a Professor of Electrical Communication Engineering (he was the Chair of the department from March 1992 to April 1995). He held visiting appointments with the Electrical Engineering Department, Stanford University, from 1986 to 1987, March to June 1994, and March to September 1996; with the Electical and Computer Engineering Department, University of Iowa, Iowa City, from June to July 1991 and June to July 1998; and with the Research Centre Imarat, Hyderabad, from September 1995 to February 1996. He served as a consultant in the signal processing area to several research and development laboratories in Hyderabad and Bangalore. His research interests are in adaptive signal processing, multirate filtering and wavelets, space-time signal processing for wireless communication, and multicarrier modulation.

Prof. Reddy is a Fellow of the Indian Academy of Sciences, the Indian National Academy of Engineering, the Indian National Science Academy, and the Institution of Electronics and Telecommunication Engineers (IETE). He received the S.K. Mitra Memorial Award from IETE in 1989 for the Best Research Paper.